JOURNAL OF VIROLOGY, Aug. 1987, p. 2489–2498
0022-538X/87/082489-10$02.00/0

Vol. 61, No. 8

5′ Long Terminal Repeats of *myc*-Associated Proviruses Appear Structurally Intact but Are Functionally Impaired in Tumors Induced by Avian Leukosis Viruses

MAUREEN M. GOODENOW* AND WILLIAM S. HAYWARD
Memorial Sloan-Kettering Cancer Center, New York, New York 10021

Received 9 March 1987/Accepted 29 April 1987

B-cell lymphomas induced in chickens infected with avian leukosis viruses are characterized by integration of the virus within the cellular *myc* locus and alteration of c-*myc* expression. Although avian leukosis viruses are intact, replication-competent retroviruses, the structures of many *myc*-associated proviruses are altered by deletions, raising the possibility that proviral defectiveness plays an essential role in oncogenesis. We found that all *myc*-associated proviruses in 21 independent tumors had deletions, which were confined to the viral genome and did not extend into adjacent cellular sequences. Deletions were not random but, in at least 85% of the *myc*-associated proviruses, involved a region near the 5′ end of the proviral genome where elements implicated in control of viral gene expression have been localized. A second class of deletions involved sequences in the 3′ half of the viral genome and included the splice acceptor site used in generating viral *env* mRNA. Both the 5′ and 3′ long terminal repeats of *myc*-associated proviruses appeared to be structurally intact in most tumors, although the 5′ long terminal repeats were not involved in expression of either U5-*myc* transcripts or detectable steady-state viral RNAs. A complex array of repeated sequence elements surrounded the junctions of the internal deletions in two *myc*-associated proviruses. The organization of the deleted proviruses was similar to that of deleted unintegrated viral molecules, consistent with a model in which deletions occurred prior to integration.

Infection of embryonic or newly hatched chickens with avian leukosis virus (ALV) results in a high frequency of B-cell lymphomas, which originate in the bursa of Fabricius usually after a latency of 4 to 10 months (44). Bursal lymphomas are characterized by ALV integration within the c-*myc* locus (15, 16, 20, 26, 32, 39, 41), primarily between the untranslated first exon and the coding exons (48, 54), in an orientation that can result in expression of c-*myc* from one of the long terminal repeats (LTRs). Consequently, most viral tumor-specific *myc* transcripts contain proviral LTR sequences (20, 41) but not c-*myc* exon 1 (54), although exceptions have been identified in some bursal lymphoma cell lines (26).

ALVs that induce bursal lymphomas in chickens are intact, replication-competent viruses that do not harbor oncogenes. Nevertheless, it has been observed that the structure of *myc*-associated proviruses is altered by deletions in most tumors (16, 33, 42, 48, 49). Thus, it has been hypothesized that proviral defectiveness plays some essential role in oncogenesis, perhaps by contributing to the altered *myc* expression found in these tumors (10, 16, 33, 42). Deletions involving the 5′ LTR of the *myc*-associated proviruses in at least two tumors have been reported by Payne et al. (41), whereas deletions that apparently include one or the other LTR have been reported for almost 35% of *myc*-associated proviruses analyzed by Robinson and Gagnon (48). If the viral 5′ LTR were deleted, the appearance of chimeric U5-*myc* transcripts in tumors could easily be explained by initiation of transcription within the 3′ LTR. Alternatively, deletions involving the 3′ LTR need not affect normal transcription from the proviral 5′ LTR, but might result in tumor-specific *myc* RNAs if intervening viral sequences were removed by splicing. Such a mechanism has been proposed to account for the presence of LTR sequences on *myc* RNAs in the RP9 cell line, in which the 3′ LTR of the *myc*-associated provirus is deleted (39).

However, it appears that both LTRs are present in approximately 40% of deleted *myc*-associated proviruses (48), suggesting that LTR deletion may not always be a factor in ALV-induced tumorigenesis and raising the question of which LTR functions in the appearance of tumor-specific U5-*myc* transcripts. Downstream RNAs identified in two ALV-induced lymphomas have been proposed to initiate within the 3′ LTRs of internally deleted *myc*-associated proviruses in which the 5′ LTRs are intact (21). Moloney murine leukemia viruses (M-MuLVs) integrated within the c-*myb* locus in mouse myeloid tumor cells also have internal deletions involving various extents of viral *gag*, *pol*, or *env* regions but not the LTRs (52, 53). Nevertheless, tumor-specific U5-*myb* transcripts clearly originate within the 5′ LTR of the *myb*-associated MuLV and are processed to remove downstream viral and *myb* intron sequences (52). Novel RNA processing of transcripts initiated within the 5′ LTR of proviruses integrated within the c-*erbB* locus results in U5-*erbB* RNAs, although deletions of proviral sequences are not involved in ALV-induced erythroblastosis (35). The possibility that some *myc*-associated proviruses are intact and unaltered by deletion has not been completely ruled out (16, 33, 42, 48, 60). Furthermore, whether U5-*myc* RNAs in tumors originate within the 5′ or 3′ LTR of *myc*-associated proviruses with both LTRs has not been extensively explored.

We have examined in detail the organization of 21 *myc*-associated proviruses to assess the incidence of proviral deletions, to define the extent and nature of the deletions, and to determine the effect that deletions may have on provirus and *myc* expression in ALV-induced tumors. We found that all the *myc*-associated proviruses had deletions,

* Corresponding author.

which were confined to the viral genome and did not extend into the adjacent c-*myc* locus. *myc*-associated proviruses contained both 5′ and 3′ LTR sequences in most of the tumors. Nevertheless, analysis of tumor RNAs indicated that the 5′ LTRs of internally deleted *myc*-associated proviruses were not functional in expression of either detectable steady-state viral RNAs or tumor-specific U5-*myc* transcripts. Organization of the *myc*-associated proviruses was consistent with a model in which deletions occurred prior to integration.

MATERIALS AND METHODS

DNA extraction, endonuclease restriction digestion, and nucleic acid blot hybridization. ALVs and most of the tumors used in this study have been described previously (33, 55, 56). High-molecular-weight DNA or RNA was extracted from 0.5 to 1.0 g of tumor tissue (28) which had been quick-frozen in liquid nitrogen and stored at −70°C. Tumor DNAs were digested to completion with restriction endonucleases under conditions recommended by the suppliers (Bethesda Research Laboratories, Boehringer Mannheim, and New England BioLabs), electrophoresed in 0.7% agarose gels in Tris-borate-EDTA buffer, and transferred to NYTRAN membranes (Schleicher & Schuell Co.) (57). Polyadenylated [poly(A)$^+$] RNA was selected by oligo(dT) chromatography, glyoxal treated, and electrophoresed in 1% agarose gels in 10 mM phosphate buffer (pH 6.8) prior to transfer to NYTRAN (29, 61).

After being dried in a vacuum oven for 1.5 h at 80°C, filters were prehybridized at 65°C for 6 h with solutions containing 6× SSC (1× SSC is 0.15 M NaCl plus 0.015 M sodium citrate), 2× Denhardt solution (1× Denhardt solution is 0.02% bovine serum albumin, 0.02% Ficoll, and 0.02% polyvinylpyrrolidine), 0.5 mg of yeast RNA per ml, 50 mM sodium phosphate (pH 6.8), and 1% sodium dodecyl sulfate (SDS). Blots were hybridized at 65°C for 18 h with 10^6 Cerenkov cpm of ^{32}P-labeled probe per ml of prehybridization solution containing 5% dextran sulfate. Filters were washed twice for 15 min each at room temperature and twice for 60 min each at 65°C in 0.1× SSC–0.1% SDS. XAR-5 film and intensifying screens were used for autoradiography. Filters were placed in boiling H_2O for 20 to 30 min and autoradiographed for 5 to 7 days before hybridization with another probe.

Preparation of ^{32}P-labeled DNA probes. High-specific-activity probes (>10^9 Cerenkov cpm/μg of DNA) were prepared by incorporation of [α-^{32}P]dCTP (3,000 Ci/mmol; New England Nuclear Corp.) into double-stranded DNA (13). The following c-*myc* probes were used: a 1.1-kilobase (kb) *Sma*I subclone that includes exon 1; a 0.4-kb *Sma*I subclone which contains the 5′ region of intron 1; a 0.47-kb *Sma*I-*Pst*I subclone that includes the 3′ region of intron 1 and a small portion of exon 2; and an 848-base-pair (bp) *Cla*I-*Eco*RI fragment which contains most of exon 3. Viral probes included U5L, a 315-bp *Eco*RI-*Sac*I subclone of plasmid p5′NCR (from E. Stavnezer); U5, a 170-bp *Eco*RI-*Bst*EII suclone of pU5L; LDR, a 175-bp *Bst*EII-*Sac*I subclone of pU5L; U3, a 450-bp *Pvu*II-*Eco*RI fragment from plasmid p3′NCR (from E. Stavnezer); p*gag*, a 2.0-kb *Sac*I-*Eco*RI subclone of Rous-associated virus type 2 (RAV-2); and p*pol*, a 2.6-kb *Eco*RI-*Kpn*I subclone of RAV-2.

Cloning tumor DNA and analysis of phage clones. Tumor DNA was digested to completion with *Sac*I and size fractionated on sucrose gradients (28). DNA from appropriate fractions was ligated into *Sac*I-digested λ2001 cloning vector (24) and packaged in vitro. Libraries containing 5 × 10^5 to 1 × 10^6 recombinant phage were amplified once before screening with the exon 1 and U5L probes (5). Inserts from recombinant phage were first subcloned into pUC plasmids for restriction analysis. Appropriate fragments were subcloned into mp18 and mp19 bacteriophage M13 vectors (31, 68) for sequencing by the dideoxy chain termination method (50).

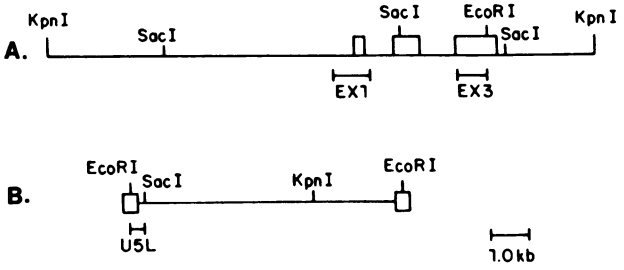

C.

No. of tumors	Unique Proviral Restriction Sites: SacI	KpnI
10	-	+
3	-	-
2	-	NT
3	+	+
3	+	-

FIG. 1. Restriction endonuclease sites in the avian c-*myc* locus, ALV genome, and *myc*-associated proviruses used in these analyses. (A) The avian c-*myc* locus contains three exons (32, 36, 47, 63). A 7.0-kb *Sac*I fragment is detected with an exon 1 (EX1) probe, while a 16.0-kb *Kpn*I fragment is detected with exon 1 and exon 3 (EX3) probes. (B) The 7.8-kb ALV proviral genome contains a *Sac*I site almost 500 bp from the 5′ end and a *Kpn*I site within its 3′ region. The U5L probe extends from *Eco*RI to *Sac*I at the 5′ end of the genome. (C) *myc*-associated proviruses in 21 ALV-induced tumors were examined for the presence of proviral *Sac*I and *Kpn*I restriction enzyme sites. Symbols: −, site absent; +, site present; NT, not tested.

RESULTS

Deletions in *myc*-associated proviruses. The 21 tumors analyzed in these studies were induced with either RAV-1, RAV-2, RP9, UR2-associated virus (UR2AV), ring-necked pheasant virus (RPV), RU9, or transformation-defective mutants of the Schmidt-Ruppin strain of Rous sarcoma virus (RSV). Seventeen of these tumors were shown previously to contain tumor-specific proviruses integrated upstream of c-*myc* exon 2 (32, 54, 56). In the course of the present experiments, *myc*-associated proviruses in four additional tumors were mapped 3.1 to 3.4 kb upstream of the *Eco*RI site in c-*myc* exon 3 (Fig. 1A). Among the 21 tumors, proviruses were located within intron 1 in 15 tumors, within exon 1 in 4 tumors, or just upstream of exon 1 but within a region detectable by the exon 1 probe in 2 tumors. Proviral integrations in all but tumor 41 were in the same transcriptional orientation as the c-*myc* gene (54).

The genomes of ALV proviruses are approximately 7.8 kb long and contain a unique *Sac*I restriction endonuclease site

near their 5′ end and a unique *Kpn*I restriction site just upstream of the splice acceptor site in *env* (Fig. 1B). It was possible to estimate the size of the provirus integrated within the c-*myc* locus by hybridizing *Sac*I-digested or *Kpn*I-digested tumor DNAs with c-*myc* exon 1 and exon 3 probes and an ALV U5L probe (Fig. 1).

In 15 tumors, altered *Sac*I fragments, which were 2.0 to 7.0 kb larger than the 7.0-kb *Sac*I fragment of the normal c-*myc* allele, were detected with the exon 1 and U5L probes. These results indicated that the ALV *Sac*I site was missing in more than 70% of the *myc*-related proviruses (Fig. 1C). In most of these tumors (10 of 15), the *myc*-associated proviral *Kpn*I site was present, but a portion of the proviral sequences 5′ of it were deleted. Three tumors contained *myc*-associated proviruses in which neither the ALV *Sac*I nor *Kpn*I site was detected, indicating deletions involving more than half of the viral genome.

In almost 30% of the tumors (6 of 21), altered c-*myc* *Sac*I fragments that were very similar in size to the normal 7.0-kb c-*myc* *Sac*I fragment were detected with the exon 1 and U5L probes. It was possible that these altered *Sac*I fragments reflected the presence of a single LTR (330 bp) within the c-*myc* locus. Alternatively, in tumors with proviruses integrated 200 to 700 bp upstream of the *Sac*I site in c-*myc* exon 2, the 6.8- to 7.3-kb altered *Sac*I fragments might be due to the presence of the proviral *Sac*I restriction site together with the 500 bp of viral sequences 5′ of it (Fig. 1B). The results of analysis of *Kpn*I-digested tumor DNAs with the exon 1 and exon 3 probes were consistent with the latter alternative (Fig. 1C). Both c-*myc* probes hybridized to a normal 16.0-kb *Kpn*I fragment. In three tumors (36, 32, and 33), additional *Kpn*I fragments, which differed in size from each other and were smaller than the normal *Kpn*I fragment, were detected with the exon 1 and exon 3 probes. These results indicated the presence of the proviral *Kpn*I site. Based on the size of the altered *Kpn*I fragments, it was possible to localize the deletions in the *myc*-associated proviruses to the region between the ALV *Sac*I and *Kpn*I restriction sites (Fig. 2). In the remaining three tumors (45, 419, and 373), a single *Kpn*I fragment, which was larger than the normal fragment, hybridized with both c-*myc* probes. These results suggested that about 3.0 to 4.0 kb of the *myc*-associated proviruses, including the proviral *Kpn*I sites, were deleted (Fig. 2).

This series of experiments indicated that all *myc*-associated proviruses in ALV-induced tumors had deletions and that the deletions ranged from approximately 1.0 to 6.0 kb of the viral genome. However, these results did not rule out the possibility that the deletions in 15 proviruses that lacked the *Sac*I site extended beyond the 5′ proviral boundaries into adjacent host sequences or that additional rearrangements of either the c-*myc* locus or *myc*-associated proviral sequences had occurred in any of the tumors.

Organization of *myc*-associated proviruses. To determine in more detail the organization of *myc*-associated proviruses, 21 c-*myc* alleles altered by proviral integration in ALV-induced tumors were examined by extensive restriction analysis and hybridization with both c-*myc* and viral probes (see Materials and Methods). The absence of the ALV-specific *Sac*I site in 15 *myc*-associated proviruses raised the possibility that the 5′ LTR might have been deleted. However, 5′ LTR sequences were demonstrated directly in 12 *myc*-associated proviruses by the presence of either *Pvu*I or *Eco*RI restriction sites within the LTR (Fig. 2). Moreover, in these tumors and in tumor 28, 5′ cell-virus junction fragments generated by other restriction enzymes were

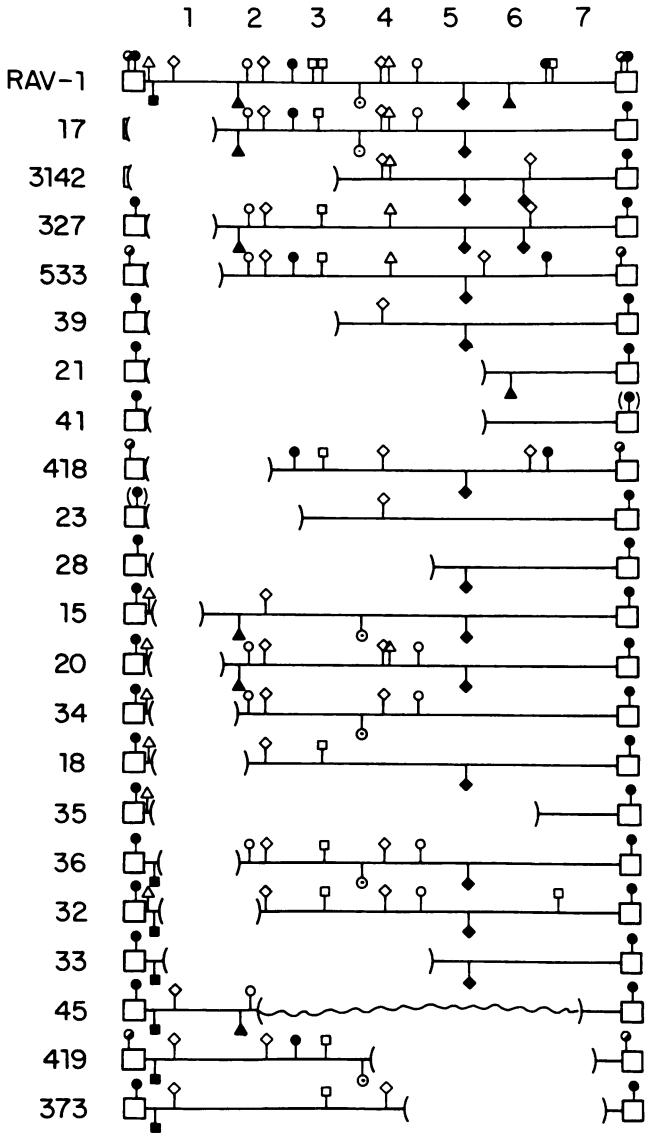

FIG. 2. Organization of *myc*-associated proviruses in 21 ALV-induced tumors. RAV-1 was used to induce tumors 18, 32, 33, 34, 35, 36, and 39; *td*107a and *td*109 (transformation-defective variants of Schmidt-Ruppin A strain RSV) (64), tumors 17, 20, 21, and 28; RAV-2, tumors 15 and 23; RAV-2-related virus from RP9 cell line, tumor 45; RPV, tumors 327, 373, and 3142; UR2AV, 418 and 419; RU9 (an in vitro recombinant in which all of *gag* and most of *pol* or UR2AV were replaced with the analogous regions from RPV) (55), tumor 533. All proviruses, except that in tumor 41, integrated in the same transcriptional orientation as c-*myc*. Restriction sites among the viruses are essentially identical in *gag* and *pol* regions; polymorphism occurs in *env*. Symbols represent restriction sites used in analysis of *myc*-associated proviruses. Deletions in the *myc*-associated proviruses are indicated by parentheses. 5′ LTR sequences of the *myc*-associated proviruses in tumors 17 or 3142 were not detected by restriction analysis of genomic DNA with viral U3 or U5 probes. A portion of the 5′ LTR was found when the *myc*-associated provirus in tumor 17 was cloned and the 5′ cellular-viral junction was sequenced (see Results). Results of restriction analyses of the *myc*-associated provirus in tumor 3142 were consistent with the possibility that some LTR sequences remain at its 5′ end. Symbols: ∿, region in the *myc*-associated provirus in tumor 45 that could not be resolved by analysis of genomic DNA (see Results); ◇, *Bam*HI; ▲, *Bgl*I; ○, *Bgl*II; △, *Bst*EII; ●, *Eco*RI; □, *Hind*III; ◆, *Kpn*I; ◑, *Pvu*I; ■, *Sac*I; ⊙, *Xba*I.

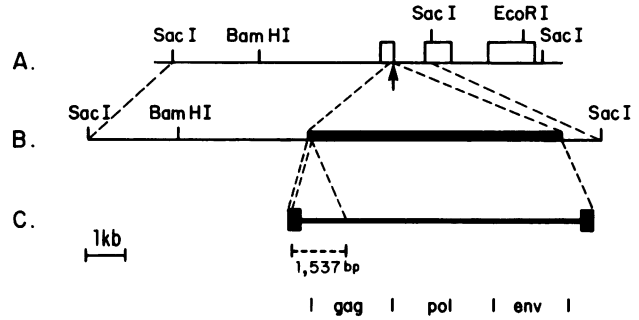

FIG. 3. Organization of the *myc* allele altered by proviral integration in tumor 17. (A) Normal avian c-*myc* allele. (B) *Sac*I fragment cloned from tumor 17 includes a deleted *myc*-associated provirus (solid box) with 5'- and 3'-flanking cellular sequences. The provirus is integrated within the 3' region of c-*myc* exon 1. (C) *myc*-associated provirus has an internal deletion of 1,537 bp of viral sequences, including most of the 5' LTR and adjacent *gag* sequences.

detected with both the c-*myc* exon 1 and ALV U5L probes. However, there was no evidence by these criteria for 5' LTR sequences in either tumor 17 or tumor 3142.

The organization of approximately 25 kb of flanking cellular DNA from each tumor-specific c-*myc* allele was assessed by digestion with a number of restriction enzymes and hybridization with probes extending over 4.5 kb of the c-*myc* locus. Neither rearrangement nor deletion of cellular *myc* sequences flanking the integrated provirus was detected in any tumor (data not shown).

These experiments suggested, for all but tumors 17 and 3142, that deletions were confined to the viral genome and that both 5' and 3' LTR sequences of *myc*-associated proviruses were present. In general, deletions were not random but in 85% of the tumors included a common region around the *Bam*HI site close to the 5' end of the provirus. A second class of proviral deletions involving the 3' half of the viral genome were identified. With the exception of tumor 45, the deletions appeared to involve contiguous regions of the viral genome and were not associated with other proviral rearrangements. Analyses of the *myc*-associated provirus in tumor 45 genomic DNA suggested that two separate regions of the viral genome might be deleted or that a single deletion might be associated with an inversion of viral sequences.

To determine whether the 1.5-kb deletion in tumor 17 extended into adjacent cellular sequences and to resolve the puzzling results for tumor 45, the *myc*-associated proviruses together with flanking cellular sequences were cloned from both tumors.

Organization of the *myc*-associated provirus in tumor 17. Tumor 17 was induced by *td*107A, a replication-competent deletion mutant of RSV, which is transformation defective because of loss of the v-*src* gene (64). Restriction analysis of tumor DNA showed that the *myc*-associated provirus was integrated near the 3' end of exon 1 and that the proviral *Sac*I restriction site was deleted. Therefore, the altered *myc* allele was cloned as a 13.5-kb *Sac*I fragment that included the provirus plus 5'- and 3'-flanking cellular sequences (Fig. 3). Sequencing across the 5' cellular-viral junction revealed that 61 bp at the extreme 5' end of U3 were present and joined to the proviral *gag* region as a result of a 1,537-bp deletion of viral sequences (Fig. 4). Although most of the 5' LTR was deleted, the sequence of the 3' LTR was intact (data not shown). Characteristic of integrated proviruses, 2 bp were missing from the distal ends of both LTRs and a 6-bp direct repeat of cellular sequences (nucleotides 1394 to 1399 [54]) flanked the provirus (Fig. 4). From these data, it was clear that in tumor 17 the deletion was confined to proviral sequences and did not extend into the adjacent c-*myc* locus.

Three sequence motifs appeared in both the U3 and *gag* regions surrounding the deletion junctions in tumor 17: direct repeats, inverted repeats, and palindromic repeats (Fig. 4). Long direct repeats with considerable homology (12 of 15 bp identical) flanked the deleted region. Short direct repeats were present in U3 and *gag* close to the junction formed by the deletion. As a result of the deletion, a 7-bp sequence in U3 was juxtaposed to an inversion of an almost identical sequence (6 of 7 bp) in the *gag* region. Two arrangements of palindromic sequences appeared within the 5' and 3' boundaries of the deletion. Short palindromes, present in U3 and in *gag*, were partially removed by the deletion. However, long palindromes (13 of 19 bp identical), originally located more than 1.5 kb apart in the U3 and *gag* regions of the intact virus, were brought within 10 bp of each other in the deleted provirus. It is possible that the repeated sequence elements play some role in generation of the deletions (see Discussion).

Organization of the *myc*-associated provirus in tumor 45. Tumor 45 resulted from infection by a subgroup B retrovirus (33) that had been isolated from a cell line (RP9) derived from a RAV-2-induced lymphoma (37). One proviral integration in tumor 45 mapped to within 50 bp of c-*myc* exon 2, but it was not clear from restriction analysis whether the integration site was 5' or 3' of the intron-exon boundary. Although both 5' and 3' LTR U5 regions, as well as the proviral *Sac*I site, were present, there appeared to be a deletion of approximately 4 kb of viral sequences. However, neither the precise extent nor the region(s) of the provirus deleted could be determined by restriction analysis of tumor genomic DNA.

Recombinant phage containing the altered *myc* allele and proviral sequences were isolated from a bacteriophage λ library generated from *Sac*I-digested tumor DNA. The 5' host-virus junction was contained on a 7.3-kb *Sac*I fragment that included 6.8 kb of upstream cellular sequences plus 500 bp of the *myc*-associated provirus (Fig. 5). The 3' junction was contained on a 4.0-kb *Sac*I fragment which included the proviral 3' LTR and c-*myc* sequences extending into exon 2 (Fig. 5).

Sequencing across the host-virus junctions revealed that the proviral integration had occurred 20 bp upstream of c-*myc* exon 2 and was accompanied by the characteristic loss of 2 bp at the distal end of each LTR and a 6-bp duplication of cellular sequences immediately flanking the integration site (nucleotides 2227 to 2232 [54]) (Fig. 5D). The sequence at the 5' end of the *myc*-associated provirus was intact through the viral *Sac*I site (data not shown) and similar to the same region of RAV-2 (23) except for several base changes and two major differences (Fig. 5D). The U3 region of the provirus from tumor 45 contained 10 bp that were not present in RAV-2. In addition, an 11-bp sequence, which includes a core sequence common to a number of enhancer elements (25) and which ordinarily appears twice in the LTR U3 region of RAV-2 (23), was found in triplicate in the provirus from tumor 45. The sequence of the 3' LTR was identical to that of the 5' LTR (data not shown).

A deletion of about 4.0 kb in the *myc*-associated provirus in tumor 45 included most, if not all, of the *pol* and *env* genes. Approximately 1.5 kb of viral *gag* sequences 3' of the

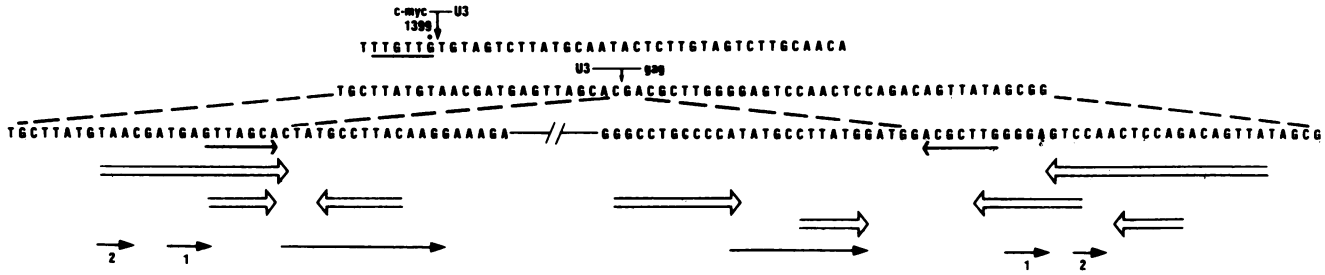

FIG. 4. Partial sequence of the *myc*-associated provirus in tumor 17. Sequence of the 5′ host-virus junction (top line). The integrated provirus has lost 2 bp at the distal end of each LTR and is flanked by a 6-bp direct repeat of cellular sequences (underlined). Sequence across the deletion (second line). U3 and *gag* sequences (51, 58, 59) surrounding the deletion junctions contain a number of repeated sequence elements (third line). Symbols: ⟶, inverted repeats; ⇒, palliondromes; ⟶, direct repeats.

viral SacI site were detected by restriction analysis of tumor genomic DNA (Fig. 2) but were not included on the cloned 3′ *Sac*I fragment (Fig. 5B). Unexpectedly, at least 3.0 kb of the sequences between the proviral LTRs were not viral (Fig. 5B) but were homologous with cellular sequences normally present in single copy in the haploid avian genome (M. M. Goodenow, unpublished results). Thus, the structure of the *myc*-associated provirus in tumor 45 apparently resulted from incorporation of a unique region from the avian genome in place of the 3′ region of the retrovirus and represents a novel organization for a *myc*-associated provirus in ALV-induced lymphomas.

Expression of *myc*-associated proviruses. Both 5′ and 3′ LTRs of deleted *myc*-associated proviruses appeared to be structurally intact in most of the tumors, raising the possibility that the 5′ LTR may be functional either in viral expression or in tumor-specific *myc* expression or both. Expression of *myc*-associated proviruses with structurally intact 5′ LTRs should result in viral transcripts ranging in size from approximately 2.0 to 6.0 kb, depending on the extent of proviral deletions. Such transcripts would include U5 sequences but may or may not contain leader sequences, depending on the location of deletions within the provirus (Fig. 2). In addition to *myc*-associated proviruses, ALV-induced tumors frequently have other exogenous proviruses (20, 33, 34, 42, 48) which may be intact. Normal proviral expression results in two major poly(A)$^+$ RNA species of approximately 8.0 and 3.0 kb, representing full-length and *env* transcripts, respectively (19, 30, 66). Each viral RNA contains both U5 and leader sequences.

To detect transcripts reflecting the organization of *myc*-associated proviruses, poly(A)$^+$ RNAs from 13 tumors were analyzed by Northern (RNA) blotting with two probes, one specific to the U5 region of the LTR and the other specific to the ALV leader region (LDR probe) (Fig. 6A). Both probes detected 8.0- and 3.0-kb viral RNAs, consistent with the

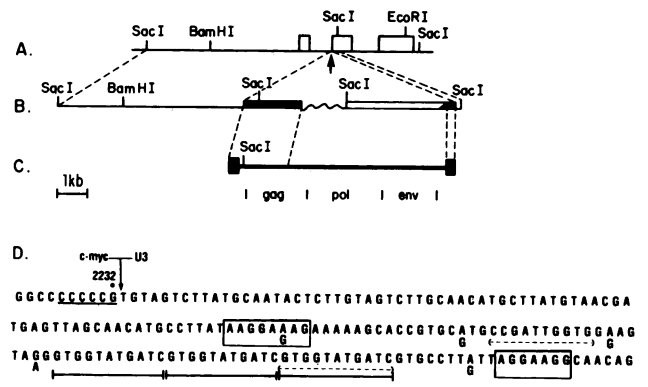

FIG. 5. Organization of the *myc* allele altered by proviral integration in tumor 45. (A) Normal avian c-*myc* allele. (B) Altered c-*myc* allele contains a provirus integrated 20 bp upstream of the c-*myc* exon 2 boundary. The provirus has a deletion of approximately 4.0 kb of viral sequences but includes single-copy sequences from the avian genome (open box). The 3′ boundary between the genomic and viral sequences, indicated by a diagonal line, has not been precisely determined by sequencing. The wavy line indicates that a portion of the internal sequences were not obtained due to the cloning strategy. (C) *myc*-associated provirus (solid box) includes both 5′ and 3′ LTRs, as well as most of *gag* and a portion of *env*. (D) Sequence of the 5′ cellular-viral junction shows a loss of the distal 2 bp of LTR sequences and a 6-bp duplication of cellular sequences (underlined). The sequence of U3 is essentially the same as RAV-2 (23), the presumed progenitor virus. Nucleotide differences in RAV-2 are indicated under the sequence of the *myc*-associated provirus. Symbols: (----), sequences not found in U3 of RAV-2; boxes, sequences implicated as enhancer elements (25); ⊢⊣, region with sequence homology to core enhancer elements which appears only twice in RAV-2.

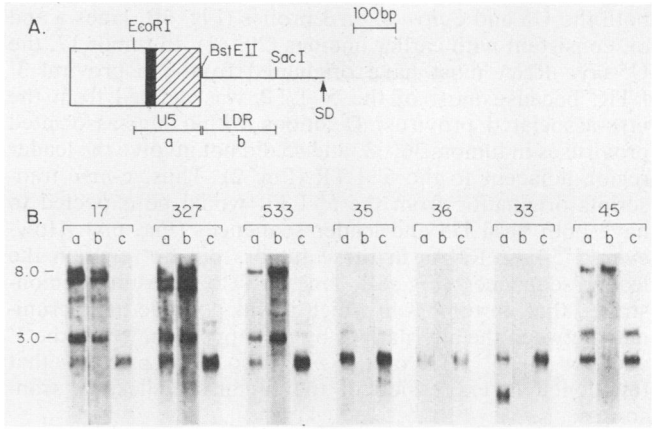

FIG. 6. Analysis of tumor poly(A)$^+$ RNAs for expression of *myc*-associated proviruses and tumor-specific *myc* transcripts. (A) The 5′ LTR contains U3 (□), R (■), and U5 (▨). The leader region (—) extends from the *Bst*EII site to the splice donor (SD) sequence. The U5 (a) and LDR (b) probes were generated by subcloning *Eco*RI-*Bst*EII and *Bst*EII-*Sac*I fragments of the 5′ LTR of RAV-2. Subcloned fragments were purified from polyacrylamide gels and labeled to high specific activity by the random priming method (13). (B) Poly(A)$^+$ RNA (5 μg per lane) from the indicated tumors was hybridized sequentially with the U5 (lanes a), LDR (lanes b), and c-*myc* exon 3 (lanes c) probes. Sizes are indicated (in kilobases) to the left.

presence and expression of intact ALVs, in eight tumors, including tumors 17, 327, and 533 (Fig. 6B, lanes a and b). Additional viral transcripts of about 6.0 to 7.5 kb were identified with both probes in tumors 17 and 327, suggesting that defective proviruses were also present and expressed. However, the organization of *myc*-associated proviruses in these tumors precluded them as the source of the additional transcripts (Fig. 2). In four tumors, including tumors 35, 36, and 33 (Fig. 6B), there were no detectable RNAs that hybridized with both the U5 and LDR probes. The deletions in the *myc*-associated proviruses in tumors 36 and 33 did not involve the portion of the leader region defined by the LDR probe (Fig. 2). If steady-state transcripts had originated from the 5′ LTRs in these deleted proviruses, they would be expected to hybridize with both the U5 and LDR probes. In tumor 45, the entire 5′ region of the *myc*-associated provirus was intact. However, the only transcript with both U5 and leader sequences was 8.0 kb long (Fig. 6B), which was larger than the 6.5-kb RNA predicted from the organization of this provirus.

These experiments demonstrated that viral transcripts reflecting the organization of *myc*-associated proviruses were not apparent in any tumor. Thus, the 5′ LTRs of internally deleted *myc*-associated proviruses did not appear to be functional in expression of detectable steady-state viral RNAs.

Tumor-specific *myc* expression. ALV-induced tumors have been shown to express tumor-specific *myc* transcripts, which generally contain both viral U5 and c-*myc* coding sequences (20, 41) but not the untranslated first c-*myc* exon (54). It has been suggested that transcription of the altered c-*myc* allele initiates from the 3′ LTR of the *myc*-associated provirus (20). However, the presence of both 5′ and 3′ LTRs in most *myc*-associated proviruses raised the question of whether the 5′ LTR might function in expression of *myc* RNAs in any tumor.

Tumors analyzed in these studies for expression of *myc*-associated proviruses contained at least one species of RNA, varying from about 2.1 to 2.3 kb, which was detected with both the U5 and c-*myc* exon 3 probes (Fig. 6B, lanes a and c), consistent with earlier findings (20, 41). In tumor 17, the U5-*myc* RNA must have originated from the proviral 3′ LTR, because most of the 5′ LTR was deleted from the *myc*-associated provirus. Deletions within *myc*-associated proviruses in tumors 36, 33, and 45 did not involve the leader region adjacent to the 5′ LTR (Fig. 2). Thus, c-*myc* transcripts originating from the 5′ LTR would be expected to have both viral U5 and leader sequences (Fig. 6A). However, U5-*myc* RNAs in these tumors did not contain the leader sequences (Fig. 6B, lane b). These results demonstrated that, in tumors in which it was possible to discriminate between the alternatives by this approach, it was the 3′ and not the 5′ LTR of the *myc*-associated provirus that functioned in expression of the tumor-specific *myc* transcripts.

Many *myc*-associated proviruses contained 5′ LTRs that appeared to be intact, but had deletions of their leader regions. Thus, it was not possible to determine by hybridization with the LDR-specific probe which LTR functioned in expression of U5-*myc* transcripts in these tumors, including tumors 327, 533, and 35 (Fig. 6B). However, the absence of any detectable viral transcripts reflecting the organization of *myc*-associated proviruses in these tumors suggested that their 5′ LTRs were functionally impaired. Mutations or deletions which affect the promoter function of the 5′ LTR have been shown to activate transcription from the 3′ LTR (10). Therefore, it seems likely that expression of U5-*myc* transcripts in tumors 327, 533, and 35 is under control of the 3′ LTR of the *myc*-associated proviruses.

Additional U5-*myc* RNAs of approximately 3.1 to 3.2 kb were detected in tumors 35 and 45 (Fig. 6B, lanes a and c). The *myc*-associated provirus in tumor 45 was positioned by sequencing to 20 bp 5′ of c-*myc* exon 2 (Fig. 5D); the provirus in tumor 35 was mapped to the same region by restriction analysis (54). The larger transcripts may represent unspliced precursors of the major 2.4-kb U5-*myc* RNA. Alternatively, the larger U5-*myc* transcripts may have initiated within sequences upstream of the *myc*-associated proviral 3′ LTR or terminated farther downstream of c-*myc* exon 3.

DISCUSSION

Organization of *myc*-associated proviruses. Our results demonstrated that all *myc*-associated proviruses in 21 independent ALV-induced lymphomas contained deletions, which were confined to viral sequences, with no detectable rearrangements or deletions within approximately 25 kb of flanking cellular DNA. Deletions were independent of the transcriptional orientation of the provirus. The *myc*-associated proviruses in tumors 41 (Fig. 2) and LL3 (67) were integrated in the opposite transcriptional orientation relative to c-*myc*. Nevertheless, their internal organization was indistinguishable from that of proviruses integrated in the same transcriptional orientation.

Although deletions ranged from 15 to 75% of the 7.8-kb proviral genome, they were not random. In most tumors (18 of 21), deletions involved a region near the 5′ end of the proviral genome, where sequences essential for initiation of retroviral replication, expression of the viral genome, and packaging of viral RNA into virions are located. Our studies revealed a second class of deletions in *myc*-associated proviruses. In three tumors, deletions were localized to the 3′ half of the provirus and included the splice acceptor site used in generating viral *env* mRNA.

Effect of proviral deletions on virus and *myc* gene expression. Whether localized to the 5′ or 3′ region of the viral genome, all deletions found in the *myc*-associated proviruses would be expected to affect expression of one or more of the viral genes because of disrupted coding sequences or splicing signals. However, deletions involving viral structural genes should not necessarily preclude transcription from the 5′ LTR, which appeared to be intact in many *myc*-associated proviruses. Thus, the absence of detectable viral or *myc* transcripts initiated from the 5′ LTR of *myc*-associated proviruses was unexpected. It is possible that the promoter activities of the proviral 5′ LTR were compromised by point mutations or small deletions. The 5′ LTRs of *myc*-associated proviruses in two tumors, LL3 (67) and 45 (this study), have been sequenced and, although not identical with the LTRs of their progenitor ALVs, appear to be essentially intact. In fact, the sequence of the 5′ LTR of the *myc*-associated provirus in tumor 45 contained an additional copy of a putative enhancer element in the U3 region and was identical to that of the 3′ LTR, which was transcriptionally active. Other studies, using chicken syncytial virus, have shown that both LTRs of an internally deleted *myc*-associated provirus are transcriptionally active in vitro (46). Therefore, in the absence of direct functional analysis in vivo, sequence alterations in the LTR do not provide a convincing explanation for the absence of detectable expression from the 5′ LTRs of *myc*-associated proviruses.

A more likely explanation for the absence of 5′ LTR-initiated transcripts is the deletion of proviral sequences thought to play a role in regulating viral gene expression. Viral sequences adjacent to the 5′ LTR have been implicated in establishing an environment that influences either the promoter function of the 5′ LTR or the stability of the viral mRNA (1, 6, 21, 25, 27). These sequences map on either side of the 5′ *Bam*HI site, which was deleted from 17 of the 21 *myc*-associated proviruses in our study. Transcripts initiated in the 5′ LTR are at least 50-fold more abundant than those from the 3′ LTR in virally infected, nontransformed cells (21). Impaired function of the 5′ LTR could result in enhanced expression of downstream *myc* sequences from the promoter in the 3′ LTR, consistent with a model of transcriptional interference in avian retroviruses (10).

In three tumors, deletions in *myc*-associated proviruses were localized to the 3′ region of the viral genome, with no apparent involvement of the elements adjacent to the 5′ LTR. Nevertheless, the 5′ LTRs were not functional in expressing steady-state RNA, whereas the promoter capability of the 3′ LTRs was active in expressing tumor-specific *myc* RNAs. These results raise the possibility that there may be additional control elements in the 3′ region of the viral genome which affect expression from the 5′ LTR. Sequences in the c-*myc* locus may also play a role in suppression of the normal function of the *myc*-associated proviral 5′ LTR.

Role of deleted *myc*-associated proviruses in tumorigenesis. There is no evidence that the retroviruses used to induce bursal lymphomas are intrinsically unstable or unusually prone to deletion formation. In fact, RAV-1 infection of other strains of chickens results in a high frequency of erythroblastosis associated with integration of intact, biologically infectious retroviruses within the c-*erbB* locus (45). Thus, defectiveness of proviruses appears to be a critical factor in the etiology of avian tumors associated with retroviral integrations in the c-*myc* locus, as the selection for tumorigenesis in this system is invariably associated with proviral deletions.

There are several functions, which are not necessarily mutually exclusive, that proviral deletions could serve. Deletions may be essential for efficient transcription of c-*myc* from the 3′ LTR (see above). This does not, however, account for deletions in proviruses integrated in the opposite transcriptional orientation from c-*myc*. Altered *myc* expression resulting from the presence of a defective provirus within the c-*myc* locus may confer some selective growth advantage on the infected cell and its progeny, thereby mediating expansion of a preneoplastic cell population that is not expressing viral antigens.

The defect in viral gene expression resulting from the deletions could be an important factor. The absence of viral proteins may permit infected cells to elude immune surveillance, because retroviral *gag* and *env* proteins, in association with class I antigens encoded by the host major histocompatibility complex, play a role in activation of the cellular immune response (14, 22, 43). Nevertheless, it has been suggested that the bursa provides protection of infected cells from the immune system, allowing hyperplasia and concomitant development of lymphoid leukosis only within the bursa of susceptible animals (2, 3).

A critical factor may be a requirement for multiple viral infections. Absence of *env* expression from a defective *myc*-associated provirus would render a cell susceptible to further retroviral infection (65). Although the generalized viremia that develops in birds infected with ALV is transient (2), viral production persists exclusively in bursal lymphocytes for at least 9 weeks after infection (3, 4), providing the opportunity for superinfection of an expanded preneoplastic cell population. ALV-induced tumor cells frequently contain a number of proviral integrations (15, 16, 20, 33, 34, 42, 48), indicating that superinfection does occur. The long latency associated with the appearance of ALV-induced bursal lymphomas suggests that altered *myc* expression may be necessary but insufficient for complete neoplastic transformation. The presence of multiple proviral insertions raises the possibility that a subsequent event(s) in the progression of ALV-induced tumors may be virally mediated.

Origin of deletions in *myc*-associated proviruses. The multiple steps involved in the retrovirus life cycle provide a number of opportunities for deletions to occur. However, sequences located adjacent to the 5′ LTR necessary for RNA packaging and initiation of reverse transcription (62) are deleted from most *myc*-associated proviruses, indicating that deletions could not have occurred until after infection and initiation of viral DNA synthesis. Deletions could be introduced before integration by a "copy-choice" mechanism involving reverse transcriptase, during the integrative process by the virally encoded endonuclease activity, or after integration.

We cannot exclude the possibility that the deletions developed after proviral integration; however, three observations lead us to favor a preintegration event. First, we found no evidence for deletions extending into adjacent cellular sequences, which might be expected in at least some tumors if random deletions had occurred subsequent to integration. Second, sequences at the distal ends of the 5′ and 3′ LTRs required for integration were retained in all *myc*-associated proviruses, suggesting a selection for defective proviruses capable of integration. Third, deletions in most *myc*-associated proviruses begin within or near an LTR and extend into the *gag* or *pol* genes, the same general region affected by deletions in many nonintegrated viral molecules (38). These observations provide a compelling reason to consider that deletions in *myc*-associated proviruses, like deletions in unintegrated viral DNA molecules, develop before integration, mediated by either retroviral reverse transcriptase or endonuclease.

A complex array of sequence elements, which might have played some role in the deletion process, surrounded the deletion junctions in the *myc*-associated provirus in tumor 17 (Fig. 4C). One other *myc*-associated provirus (LL3) that was sequenced (67) has a deletion in a region similar to that of tumor 17, although the 5′ LTR in LL3 is intact. A comparison of the sequences adjacent to the deletions in LL3 and tumor 17 showed remarkable structural similarities (Fig. 7), although no obvious sequence homology was detected. A pattern of repeated sequence elements was also observed surrounding a deletion of M-MuLV integrated within c-*myb* (53). In addition, we found a striking similarity in the organization of deletion junctional sequences between integrated *myc*-associated proviruses and nonintegrated, defective circular viral DNA molecules formed in vivo (38) (Fig. 7).

It has been suggested that internal deletions at the 5′ end of the retroviral genome can arise before integration as a result of inappropriate cleavage by the endonuclease activity encoded within the *pol* gene (38). Inaccurate cleavage may also account for preintegrative deletions in the 3′ region of the retrovirus. The preferred site of cleavage by retroviral endonuclease maps to a unique palindromic sequence found only in covalently closed circular DNA molecules containing two tandem LTRs (9, 11, 12, 18, 40). Endonuclease cleavage

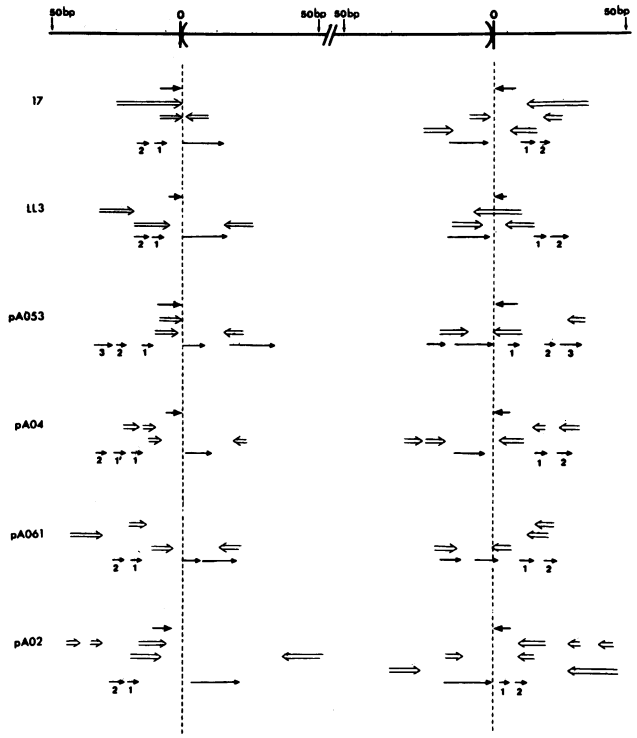

FIG. 7. Patterns of repeated sequence elements flanking deletion endpoints in two *myc*-associated proviruses (tumors 17 and LL3) and four nonintegrated viral DNA molecules (pA053, pA04, pA061, and pA02). Analysis was based on the sequence data in Fig. 4 and published data of Westaway et al. (67) and Olsen and Swanstrom (38). Symbols: 0, deletion endpoints; arrows are as described in the legend to Fig. 4.

near other palindromic sequences in the viral genome has been observed in vitro (11, 12, 18). Thus, palindromic sequences surrounding deletions in *myc*-associated proviruses may provide alternative recognition sites for endonuclease activity in vivo. Such a model, however, must account for religation of the deleted viral molecules and subsequent correct cleavage at the LTR junction before viral integration can occur.

High-frequency recombination among retroviruses, mediated by a copy-choice mechanism involving reverse transcriptase, may be facilitated by homologous repeated sequences (7). Likewise, limited sequence homology could be a factor in the formation of deletions within a retroviral genome before integration, during reverse transcription of the first DNA strand from the RNA template by a copy-choice mechanism (7), or during synthesis of the second DNA strand. A model in which deletions occur prior to integration by reverse transcriptase accounts for deletions in the 5′ or 3′ region of the viral genome and suggests a role for repeated sequence elements at the deletion junctions, although some "slippage" in the copy-choice mechanism must be invoked to explain deletions near, but not within, homologous sequences.

ACKNOWLEDGMENTS

We are grateful to Nancy Goldberg for technical assistance and Susan Perrone for preparation of the manuscript. We appreciate the helpful comments and discussion of our colleagues Norma Neff, Janet Lee, Peter Besmer, Jeffrey Greenbaum, and Madge Kanter.

This work was supported by Public Health Service grants CA-43250 and CA-16599 from the National Institutes of Health. M.M.G. was a postdoctoral fellow of the Damon Runyon-Walter Winchell Cancer Fund and a recipient of National Research Service Award CA-00740.

LITERATURE CITED

1. **Arrigo, S., M. Yun, and K. Beemon.** 1987. *cis*-Acting elements within the *gag* genes of avian retroviruses. Mol. Cell. Biol. **7**:388–397.
2. **Baba, T. W., and E. H. Humphries.** 1984. Avian leukosis virus infection: analysis of viremia and DNA integration in susceptible and resistant chicken lines. J. Virol. **51**:123–130.
3. **Baba, T. W., and E. H. Humphries.** 1985. Formation of a transformed follicle is necessary but not sufficient for development of an avian leukosis virus-induced lymphoma. Proc. Natl. Acad. Sci. USA **82**:213–216.
4. **Baba, T. W., and E. H. Humphries.** 1986. Selective integration of avian leukosis virus in different hematopoietic tissues. Virology **155**:557–566.
5. **Benton, W. D., and R. W. Davis.** 1977. Screening for λgt recombinant clones by hybridization to single plaques *in situ*. Science **196**:180–182.
6. **Broome, S., and W. Gilbert.** 1985. Rous sarcoma virus encodes a transcriptional activator. Cell **40**:537–546.
7. **Coffin, J. M.** 1979. Structure, replication, and recombination of retrovirus genomes: some unifying hypotheses. J. Gen. Virol. **42**:1–26.
8. **Coffin, J. M.** 1982. Structure of the retroviral genome, p. 261–368. *In* R. Weiss, N. Teich, H. Varmus, and J. Coffin (ed.), RNA tumor viruses. Cold Spring Harbor Laboratory, Cold Spring Harbor, N.Y.
9. **Colicelli, J., and S. P. Goff.** 1985. Mutants and pseudorevertants of Moloney murine leukemia virus with alterations at the integration site. Cell **42**:573–580.
10. **Cullen, B. R., P. T. Lomedico, and G. Ju.** 1984. Transcriptional interference in avian retroviruses—implications for the promoter insertion model of leukaemogenesis. Nature (London) **307**:241–245.
11. **Duyk, G., J. Leis, M. Longiaru, and A. M. Skalka.** 1983. Selective cleavage in the avian retroviral long terminal repeat sequence by the endonuclease associated with the αβ form of avian reverse transcriptase. Proc. Natl. Acad. Sci. USA **80**:6745–6749.
12. **Duyk, G., M. Longiaru, D. Cobrinik, R. Kowal, P. deHaseth, A. M. Skalka, and J. Leis.** 1985. Circles with two tandem long terminal repeats are specifically cleaved by *pol* gene-associated endonuclease from avian sarcoma and leukosis viruses: nucleotide sequences required for site-specific cleavage. J. Virol. **56**:589–599.
13. **Feinberg, A. P., and B. Vogelstein.** 1983. A technique for radiolabeling DNA restriction endonuclease fragments to high specific activity. Anal. Biochem. **132**:6–13.
14. **Flyer, D. C., S. J. Burakoff, and D. V. Faller.** 1983. Cytotoxic T lymphocyte recognition of transfected cells expressing a cloned retroviral gene. Nature (London) **305**:815–818.
15. **Fung, Y.-K. T., L. B. Crittenden, and H.-J. Kung.** 1982. Orientation and position of avian leukosis virus DNA relative to the cellular oncogene c-*myc* in B-lymphoma tumors of highly susceptible $15I_5X7_2$ chickens. J. Virol. **44**:742–746.
16. **Fung, Y.-K. T., A. M. Fadly, L. B. Crittenden, and H.-J. Kung.** 1981. On the mechanism of retrovirus-induced avian lymphoid leukosis: deletion and integration of the provirus. Proc. Natl. Acad. Sci. USA **78**:3418–3422.
17. **Fung, Y.-K. T., W. G. Lewis, L. B. Crittenden, and H.-J. Kung.** 1983. Activation of the cellular oncogene c-*erb*B by LTR insertion: molecular basis for induction of erythroblastosis by avian leukosis virus. Cell **33**:357–368.
18. **Grandgenett, D. P., A. C. Vora, R. Swanstrom, and J. C. Olsen.** 1986. Nuclease mechanism of the avian retrovirus pp32 endonuclease. J. Virol. **58**:970–974.
19. **Hayward, W. S.** 1977. Size and genetic content of viral RNAs in avian oncovirus-infected cells. J. Virol. **24**:47–63.

20. **Hayward, W. S., B. G. Neel, and S. M. Astrin.** 1981. Activation of a cellular *onc* gene by promoter insertion in ALV-induced lymphoid leukosis. Nature (London) **209**:475–480.
21. **Herman, S. A., and J. M. Coffin.** 1986. Differential transcription from the long terminal repeats of integrated avian leukosis virus DNA. J. Virol. **60**:497–505.
22. **Holt, C. A., K. Osorio, and F. Lilly.** 1986. Friend virus-specific cytotoxic T lymphocytes recognize both *gag* and *env* gene-coded specificities. J. Exp. Med. **164**:211–226.
23. **Ju, G., and A. M. Skalka.** 1980. Nucleotide sequence analysis of the long terminal repeat (LTR) of avian retroviruses: structural similarities with transposable elements. Cell **22**:379–386.
24. **Karn, J., W. D. Matthes, J. M. Gait, and S. Brenner.** 1984. A new selective phage cloning vector, λ2001, with sites for *Xba*I, *Bam*HI, *Hind*III, *Eco*RI, *Sst*I and *Xho*I. Gene **32**:217–224.
25. **Laimonis, L. A., P. Tsichlis, and G. Khoury.** 1984. Multiple enhancer domains in the 3′ terminus of the Prague strain of Rous sarcoma virus. Nucleic Acids Res. **12**:6427–6442.
26. **Linial, M., and M. Groudine.** 1985. Transcription of three c-*myc* exons is enhanced in chicken bursal lymphoma cell lines. Proc. Natl. Acad. Sci. USA **82**:53–57.
27. **Luciw, P. A., M. J. Bishop, H. E. Varmus, and M. R. Capecchi.** 1983. Location and function of retroviral and SV40 sequences that enhance biochemical transformation after microinjection of DNA. Cell **33**:705–716.
28. **Maniatis, T., E. F. Fritsch, and J. Sambrook.** 1982. Molecular cloning: a laboratory manual. Cold Spring Harbor Laboratory, Cold Spring Harbor, N.Y.
29. **McMaster, G. K., and G. G. Carmichael.** 1977. Analysis of single and double-stranded nucleic acids on polyacrylamide and agarose gels by using glyoxal and acridine orange. Proc. Natl. Acad. Sci. USA **74**:4835–4838.
30. **Mellon, P., and P. Duesberg.** 1977. Subgenomic cellular Rous sarcoma virus RNAs contain oligonucleotides from the 3′ half and the 5′ terminus of virion RNA. Nature (London) **270**:631–634.
31. **Messing, J., and J. Vieira.** 1982. A new pair of M13 vectors for selecting either strand of double-digest restriction fragments. Gene **19**:269–276.
32. **Neel, B. G., G. P. Gasic, C. E. Rogler, A. M. Skalka, G. Ju, F. Hishinuma, T. Papas, S. M. Astrin, and W. S. Hayward.** 1982. Molecular analysis of the c-*myc* locus in normal tissue and in avian leukosis virus-induced lymphomas. J. Virol. **44**:158–166.
33. **Neel, B. G., W. S. Hayward, H. L. Robinson, J. Fang, and S. M. Astrin.** 1981. Avian leukosis virus-induced tumors have common proviral integration sites and synthesize discrete new RNAs: oncogenesis by promoter insertion. Cell **23**:323–334.
34. **Neiman, P., L. N. Payne, and R. A. Weiss.** 1980. Viral DNA in bursal lymphomas induced by avian leukosis viruses. J. Virol. **34**:178–186.
35. **Nilsen, T. W., P. A. Maroney, R. G. Goodwin, F. M. Rottman, L. B. Crittenden, M. A. Raines, and H.-J. Kung.** 1985. c-*erbB* activation in ALV-induced erythroblastosis: novel RNA processing and promoter insertion result in expression of an amino-truncated EGF receptor. Cell **41**:719–726.
36. **Nottenburg, C., and H. E. Varmus.** 1986. Features of the chicken c-*myc* gene that influence the structure of c-*myc* RNA in normal cells and bursal lymphomas. Mol. Cell. Biol. **6**:2800–2806.
37. **Okazaki, W., R. L. Witter, C. Romero, N. Nazerian, J. M. Sharma, A. Fadley, and D. Ewart.** 1980. Induction of lymphoid leukosis transplantable tumors and establishment of lymphoblastoid cell lines. Avian Pathol. **98**:311–329.
38. **Olsen, J. C., and R. Swanstrom.** 1985. A new pathway in the generation of defective retrovirus DNA. J. Virol. **56**:779–789.
39. **Pachl, C., W. Schubach, R. Eisenman, and M. Linial.** 1983. Expression of c-*myc* RNA in bursal lymphoma cell lines: identification of c-*myc*-encoded proteins by hybrid-selected translation. Cell **33**:335–344.
40. **Panganiban, A. T., and H. M. Temin.** 1984. Circles with two tandem LTRs are precursors to integrated retrovirus DNA. Cell **36**:673–679.
41. **Payne, G. S., J. M. Bishop, and H. E. Varmus.** 1982. Multiple arrangements of viral DNA and an activated host oncogene in bursal lymphomas. Nature (London) **295**:209–214.
42. **Payne, G. S., S. A. Courtneidge, L. B. Crittenden, A. M. Fadley, J. M. Bishop, and H. E. Varmus.** 1981. Analysis of avian leukosis virus DNA and RNA in bursal tumors: viral gene expression is not required for maintenance of the tumor state. Cell **23**:311–322.
43. **Plata, F., P. Langlade-Demoyen, J. P. Abastado, T. Berbar, and P. Kourilsky.** 1987. Retrovirus antigens recognized by cytolytic T lymphocytes activate tumor rejection *in vivo*. Cell **48**:231–240.
44. **Purchase, H. G., W. Okazaki, P. K. Vogt, H. Hanafusa, B. R. Burmester, and L. B. Crittenden.** 1977. Oncogenicity of avian leukosis viruses of different subgroups and of mutants of sarcoma viruses. Infect. Immun. **15**:423–428.
45. **Raines, M. A., W. G. Lewis, L. B. Crittenden, and H.-J. Kung.** 1985. c-*erb*B activation in avian leukosis virus-induced erythroblastosis: clustered integration sites and the arrangement of provirus in the c-*erb*B alleles. Proc. Natl. Acad. Sci. USA **82**:2287–2291.
46. **Ridgeway, A. A., R. A. Swift, H.-J. Kung, and D. J. Fujita.** 1985. In vitro transcription analysis of the viral promoter involved in c-*myc* activation in chicken B lymphomas: detection and mapping of two RNA initiation sites within the reticuloendotheliosis virus long terminal repeat. J. Virol. **54**:161–170.
47. **Robbins, T., K. Bister, C. Garon, T. Papas, and P. Duesberg.** 1982. Structural relationship between a normal chicken DNA locus and the transforming gene of the avian acute leukemia virus MC29. J. Virol. **41**:635–642.
48. **Robinson, H. L., and G. C. Gagnon.** 1986. Patterns of proviral insertion and deletion in avian leukosis virus-induced lymphomas. J. Virol. **57**:28–36.
49. **Rovigatti, U. G., C. E. Rogler, B. G. Neel, W. S. Hayward, and S. M. Astrin.** 1982. Expression of endogenous oncogenes in tumor cells, p. 319–330. *In* A. H. Owens, Jr., D. S. Coffey, and S. B. Baylin (ed.), Tumor cell heterogeneity: origins and implications. Academic Press, Inc., New York.
50. **Sanger, F., A. R. Coulson, B. G. Barrell, A. J. H. Smith, and B. A. Roe.** 1980. Cloning in single-stranded bacteriophage as an aid to rapid DNA sequencing. J. Mol. Biol. **143**:161–178.
51. **Schwartz, D. E., R. Tizard, and W. Gilbert.** 1983. Nucleotide sequence of Rous sarcoma virus. Cell **32**:853–869.
52. **Shen-Ong, G. L. C., H. C. Morse III, M. Potter, and J. Frederick Mushinski.** 1986. Two modes of c-*myb* activation in virus-induced mouse myeloid tumors. Mol. Cell. Biol. **6**:380–392.
53. **Shen-Ong, G. L. C., M. Potter, J. F. Mushinski, S. Lavu, and E. P. Reddy.** 1984. Activation of the c-*myb* locus by viral insertional mutagenesis in plasmacytoid lymphosarcomas. Science **226**:1077–1080.
54. **Shih, C.-K., M. Linial, M. M. Goodenow, and W. S. Hayward.** 1984. Nucleotide sequence 5′ of the chicken c-*myc* coding region: localization of a non-coding exon that is absent from *myc* transcripts in most avian leukemia virus-induced lymphomas. Proc. Natl. Acad. Sci. USA **81**:4697–4701.
55. **Simon, M. C., W. S. Neckameyer, W. S. Hayward, and R. E. Smith.** 1987. Genetic determinants of neoplastic diseases induced by a subgroup F avian leukosis virus. J. Virol. **61**: 1203–1212.
56. **Simon, M. C., R. E. Smith, and W. S. Hayward.** 1984. Mechanisms of oncogenesis by subgroup F avian leukosis virus. J. Virol. **52**:1–8.
57. **Southern, E. M.** 1975. Detection of specific sequences among DNA fragments separated by gel electrophoresis. J. Mol. Biol. **98**:503–517.
58. **Swanstrom, R., W. J. DeLorbe, J. M. Bishop, and H. E. Varmus.** 1981. Sequencing of cloned unintegrated avian sarcoma virus DNA: viral DNA contains direct and inverted repeats similar to those in transposable elements. Proc. Natl. Acad. Sci. USA **78**:124–128.
59. **Swanstrom, R., H. E. Varmus, and J. M. Bishop.** 1982. Nucleotide sequence of the 5′ noncoding region and part of the *gag* gene of Rous sarcoma virus. J. Virol. **41**:535–541.
60. **Swift, R. A., E. Shaller, R. L. Witter, and H.-J. Kung.** 1985. Insertional activation of c-*myc* by reticuloendotheliosis virus in

chicken B lymphoma: nonrandom distribution and orientation of the proviruses. J. Virol. **54**:869–872.

61. **Thomas, P. S.** 1980. Hybridization of denatured RNA and small DNA fragments transferred to nitrocellulose. Proc. Natl. Acad. Sci. USA **77**:5201–5205.
62. **Varmus, H., and R. Swanstrom.** 1982. Replication of retroviruses, p. 369–512. *In* R. Weiss, N. Teich, H. Varmus, and J. Coffin (ed.), RNA tumor viruses. Cold Spring Harbor Laboratory, Cold Spring Harbor, N.Y.
63. **Vennstrom, B., D. Sheiness, J. Zabielski, and J. M. Bishop.** 1982. Isolation and characterization of c-*myc*, a cellular homolog of the oncogene (v-*myc*) of avian myelocytomatosis virus strain 29. J. Virol. **42**:773–779.
64. **Wang, L.-H., P. Snyder, T. Hanafusa, and H. Hanafusa.** 1980. Evidence for the common origin of viral and cellular sequences involved in sarcomagenic transformation. J. Virol. **35**:52–64.
65. **Weiss, R.** 1982. Experimental biology and assay of RNA tumor viruses, p. 209–260. *In* R. Weiss, N. Teich, H. Varmus, and J. Coffin (ed.), RNA tumor viruses. Cold Spring Harbor Laboratory, Cold Spring Harbor, N.Y.
66. **Weiss, S. R., H. E. Varmus, and J. M. Bishop.** 1977. The size and genetic composition of virus-specific RNAs in the cytoplasm of cells producing avian sarcoma-leukosis viruses. Cell **12**:983–992.
67. **Westaway, D., G. Payne, and H. Varmus.** 1984. Proviral deletions and oncogene base-substitutions in insertionally mutagenized c-*myc* alleles may contribute to the progression of avian bursal tumors. Proc. Natl. Acad. Sci. USA **81**:843–847.
68. **Yanisch-Perron, G., J. Vieira, and J. Messing.** 1985. Improved M13 phage cloning vectors and host strains: nucleotide sequence of the M13 mp18 and pUC19 vectors. Gene **33**:103–119.